

# Network Analysis Reveals Sex- and Antibiotic Resistance-Associated Antivirulence Targets in Clinical Uropathogens

Kaveri S. Parker,<sup>†,‡,§</sup> James D. Wilson,<sup>§,△</sup> Jonas Marschall,<sup>‡,§,⊥</sup> Peter J. Mucha,<sup>\*,⊗</sup> and Jeffrey P. Henderson<sup>\*,†,‡,§</sup>

<sup>†</sup>Center for Women's Infectious Diseases Research, <sup>‡</sup>Division of Infectious Diseases, and <sup>#</sup>Department of Internal Medicine, Washington University in St. Louis, St. Louis, Missouri 63110, United States

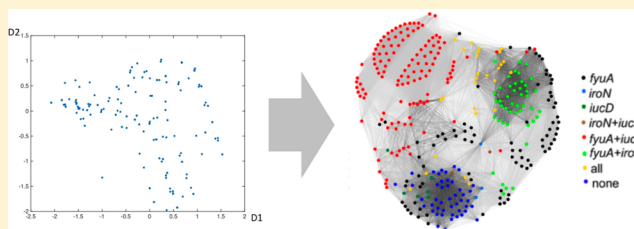
<sup>§</sup>Department of Statistics and Operations Research and <sup>⊗</sup>Carolina Center for Interdisciplinary Applied Mathematics, Department of Mathematics, University of North Carolina, Chapel Hill, North Carolina 27599, United States

<sup>⊥</sup>Department of Infectious Diseases, Bern University Hospital and University of Bern, 3010 Bern, Switzerland

## S Supporting Information

**ABSTRACT:** Increasing antibiotic resistance among uropathogenic *Escherichia coli* (UPEC) is driving interest in therapeutic targeting of nonconserved virulence factor (VF) genes. The ability to formulate efficacious combinations of antivirulence agents requires an improved understanding of how UPEC deploy these genes. To identify clinically relevant VF combinations, we applied contemporary network analysis and biclustering algorithms to VF profiles from a large, previously characterized inpatient clinical cohort. These mathematical approaches identified four stereotypical VF combinations with distinctive relationships to antibiotic resistance and patient sex that are independent of traditional phylogenetic grouping. Targeting resistance- or sex-associated VFs based upon these contemporary mathematical approaches may facilitate individualized anti-infective therapies and identify synergistic VF combinations in bacterial pathogens.

**KEYWORDS:** uropathogens, UPEC, UTI, antibiotic resistance, novel therapeutic targets, sex specificity in infections, network analysis



Antibiotic resistance is widely recognized as one of the 21st century's pre-eminent public health challenges. There is also a growing appreciation that conventional broad-spectrum antibiotic strategies exert deleterious "off-target effects" on the human microbiome.<sup>1,2</sup> Antibiotic therapies for urinary tract infections (UTIs), which are predominantly caused by uropathogenic *Escherichia coli* (UPEC), have come to exemplify both challenges. UPEC are becoming notably resistant to the potent oral trimethoprim/sulfamethoxazole and fluoroquinolones that have long been a mainstay of outpatient UTI therapy,<sup>3,4</sup> presenting an increasing healthcare burden.<sup>5</sup> Fluoroquinolone use has also been implicated in the rise of community-acquired *Clostridium difficile*, an opportunistic infection that takes root when the intestinal microbiome is disturbed by antibiotic exposure.<sup>6</sup> These shortcomings of current broad-spectrum antibiotic approaches have motivated renewed interest in precision therapeutic approaches directed against pathogen-specific molecular targets that circumvent existing resistance mechanisms and spare beneficial members of the gut microbiome. Chief among these are antivirulence agents that selectively disarm pathogenic functions in bacteria without suppressing beneficial functions of intestinal microbes.<sup>7</sup>

Prior studies, aided by UPEC's genetic tractability, have identified numerous monogenic urovirulence determinants in clinical *E. coli* isolates. Many of these genetic loci, termed

virulence factors (VFs), are nonconserved or are carried on mobile genetic elements and are known to execute specific biochemical functions related to uropathogenesis.<sup>8</sup> The biochemical functions of many VFs are known in sufficient detail to permit prototype antivirulence therapeutic agents to be identified or developed. VFs associated with iron acquisition systems (siderophores<sup>9</sup>), in particular, have been targeted by biosynthetic inhibitors,<sup>10</sup> import inhibitors, and "Trojan horse" toxins such as pesticin, albomycin, and microcins.<sup>11–14</sup> *E. coli* adhesins have also been targeted for inhibition in approaches that could be expanded to other adhesin types.<sup>15–17</sup> Continued efforts are likely to provide an expanded panel of antivirulence agents that may be combined to maximize clinical efficacy.

An important theoretical weakness of antivirulence therapies arises from the targets' potentially brief period of pathophysiologically relevant activity, which may limit an agent's efficacy. Just as uropathogenic adaptations are generally multifactorial in nature, antivirulence agents will likely have to be combined for efficacy.<sup>18,19</sup> In addition to increasing efficacy, combination drug approaches typically limit the rate at which resistant mutants emerge by forcing pathogens to develop multiple

**Special Issue:** Gram-Negative Resistance

**Received:** February 26, 2015

**Published:** July 24, 2015

simultaneous resistance adaptations. These principles underlie current combination anti-infective therapies against *Helicobacter pylori*, *Mycobacterium tuberculosis*, and HIV. Although combined siderophore and adhesin inhibitor therapy may be similarly effective against uropathogenic *E. coli*, it has been unclear how to optimally combine these agents to best treat urological infections. Currently unexplored associations between UPEC VFs further complicate combination antivirulence therapeutic formulations for UTI.

To determine which antivirulence target combinations predominate in patients, we applied mathematical network community detection and statistical biclustering to uropathogenic *E. coli* VF genotypes from a previously described hospitalized UTI patient cohort with a high incidence of antibiotic resistance, pyelonephritis, and bacteremia.<sup>20</sup> The mathematical tools used here<sup>21–23</sup> simultaneously considered VF genotypes and their frequency among 337 clinical pathogenic isolates and identified 4 stereotypical urovirulence strategists. These strategists were independently associated with antibiotic resistance and patient sex. These results provide a preliminary framework for devising and prioritizing combinatorial antivirulence strategies and support the use of these mathematical approaches to address this and other unresolved questions in infectious diseases.

## RESULTS AND DISCUSSION

**Clinical Isolate Characteristics.** Three hundred and thirty-seven bacteriuric inpatient *E. coli* clinical isolates (CIs) were derived from a recently described inpatient cohort collected over the course of one year (Table 1).<sup>20</sup> The CIs

**Table 1. Clinical Characteristics of Clinical Isolates Tested in This Study**

metric	total (%)
female	263 (78)
male	74 (22)
pyelonephritis	107 (32)
sepsis-induced hypotension (SIH)	60 (17)
bloodstream infection (BSI)	24 (7)
ciprofloxacin (CIP) resistant	117 (35)
trimethoprim/sulfamethoxazole (TMP/S) resistant	96 (29)
phylogenetic group B2	232 (68)
phylogenetic group D	54 (16)
phylogenetic group B1	41 (12)
phylogenetic group A	10 (3)

characterized in this study were predominantly female ( $n = 263$ , 78%), with a median inpatient age range of 62 years (range, 19–101 years). One hundred and seven patients had pyelonephritis (32%), 60 had sepsis-induced hypotension (17%), and 24 had bacteremia (7%). The *E. coli* phylogenetic group distribution was typical of urinary isolates, with a majority of strains contained in group B2 (68%).<sup>24</sup> One hundred and seventeen isolates were resistant to ciprofloxacin (CIP, 35%), and 96 were resistant to trimethoprim/sulfamethoxazole (TMP/S, 29%).

**Virulence Factor Distribution.** CIs were assessed for the presence or absence of 16 VF genes (Table 2) that have been collectively addressed in over 2700 publications (Figure S1). One hundred and twenty-seven unique, nonredundant VF genotypes were present among the clinical isolates examined in this study. Virulence factor prevalence ranged from highly

**Table 2. Virulence Factors and Their Functions**

gene	function
<i>chuA</i>	<i>E. coli</i> heme uptake
<i>fyuA</i>	siderophore (yersiniabactin uptake)
<i>ompT</i>	surface protease
<i>tspE</i>	anonymous DNA fragment
<i>yjaA</i>	hypothetical protein
<i>usp</i>	bacteriocin
<i>capII</i>	group II capsule antigen
<i>iucD</i>	siderophore (aerobactin)
<i>iha</i>	<i>irgA</i> homologue adhesin
<i>sat</i>	secreted autotransporter toxin
<i>prf</i>	adhesion (P-related fimbriae)
<i>iroN</i>	siderophore (salmochelin)
<i>hlyA</i>	hemolysin
<i>sfa</i>	adhesion (S-fimbriae)
<i>cnf1</i>	cytotoxic necrotizing factor
<i>Dr</i>	adhesion ( <i>Dr</i> family)

common (*chuA*; 84%) to infrequent (*Dr*; 7%, Figure 1a). Using a  $z$  test for normality, we found that the gene content is not normally distributed ( $p = 0.031$ ). Indeed, a histogram of VF

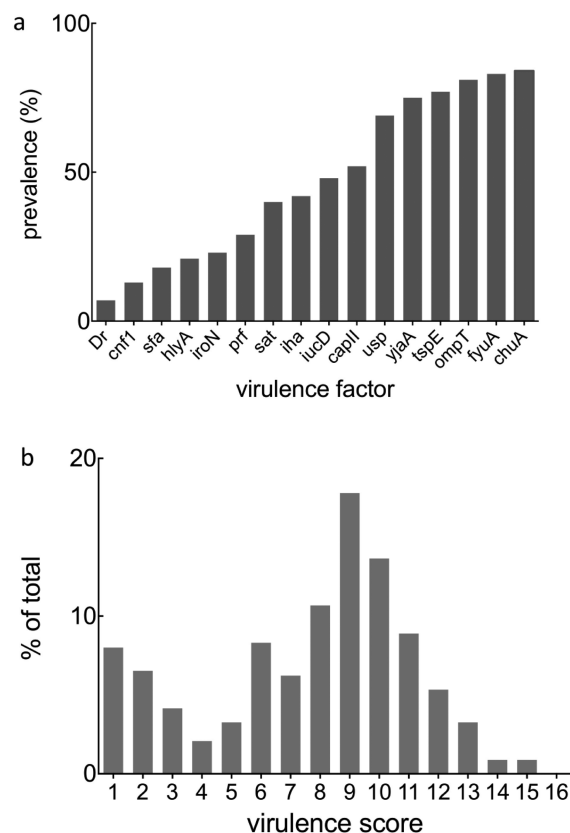


**Figure 1.** Virulence factor incidence and distribution among the clinical isolates examined in this study: (a) Virulence factor incidence in the 337 clinical isolates shown. (b) Each virulence factor (VF) was assigned a score of 1. Any virulence score  $\geq 1$  indicates the presence of one or more VFs, and 0 is the absence of individual genes. Because the presence and absence of all 16 genes were considered, the VF score ranged from 0 to 16. Next, a data matrix was generated to determine each clinical isolate's VF profile. A bimodal distribution of virulence scores was observed among 337 clinical isolates, with local maxima at one and nine virulence factors.

gene content frequency reveals a bimodal distribution with local maxima at one and nine virulence factors (Figure 1b). This bimodal distribution is consistent either with two quantitative optima for VF content or with the tendency of VFs to occur in modular combinations. An overview by principal component analysis (PCA) did not clearly resolve any coherent patterns in this data set (Figure S2).

**Network Community Detection of Uropathogenic Strategies.** To determine whether UPEC VFs are associated with each other in stereotypical patterns, we next applied modularity-based community detection to a network of the 16 VFs alone. We set weighted edges between VFs by statistically significant positive correlations (by Fisher's exact test at the 1.5% one-sided level to ensure a single component connecting all 16 VFs). Three interrelated VF communities are discernible within the resulting heatmap (Figure 2a), corresponding force-directed layout (Figure 2b), and VF nested hierarchy of communities (Figure 2c). Siderophore genes are uniquely represented in each VF community (VF community 1, *fyuA*; VF community 2, *iroN*; VF community 3, *iucD*). Weaker positive correlations between the *fyuA*-containing VF community and those containing *iucD* or *iroN* are evident in the VF adjacency matrix. Network community detection thus shows that the clinical *E. coli* isolates deploy VFs in stereotypical combinations.

**Network Community Detection of Clinical Isolates.** To determine whether UPEC carry stereotypical VF combinations, we applied modularity-based community detection to a network representation of the 337 clinical isolates. We defined a CI network of positively associated pairs after correcting for each VF's mean frequency and variance across the study population (see Methods for details). Modularity-based community detection resolves four clinical isolate communities (CI communities 1–4,  $n = 45, 118, 76,$  and  $98$ , respectively), representing four distinct virulence strategists (Figure 3a). Each community contains distinctive VF patterns that together encompass multiple functional classes. A force-directed layout of this network indicates connectivity and strength of association between UPEC isolates (Figure 3b). These stereotypical distributions suggest that virulence genes are present as modular communities from which relevant antivirulence targets can be prioritized.

**Biclustering Analysis.** As a complementary alternative to network community detection, we employed an iterative binary biclustering method based on the large average submatrix (LAS) procedure described by Shabalin et al.<sup>23</sup> Whereas network-based community detection assigns each VF or clinical isolate to a single community, biclustering simultaneously identifies highly co-occurring VFs and CIs. A CI or VF may belong to multiple biclusters (BCs) or none at all. Four BCs emerge from our clinical population (BC 1–4,  $n = 234, 112, 62,$  and  $39$ , respectively; Figure 4a), in a manner consistent with the four virulence strategists identified by network community detection. Overall, VFs associated with each bicluster are highly expressed across the constituent CIs (>72%). Biclustering did not classify 62 CIs with low VF gene content, the collection of which grossly resembles CI community 4. BC 4 is mostly redundant with BC 1 but is most distinguished by the absence of two genes (*sfa* and *cnf1*) and the low prevalence of four genes (*yjaA*, *usp*, *iroN*, and *hlyA*). The most abundant classifications resemble the CI communities, with the largest single bicluster combination (BC1+2, strains appearing in BC1 and BC2 but no other BCs,  $n = 89$ ) closely resembling CI

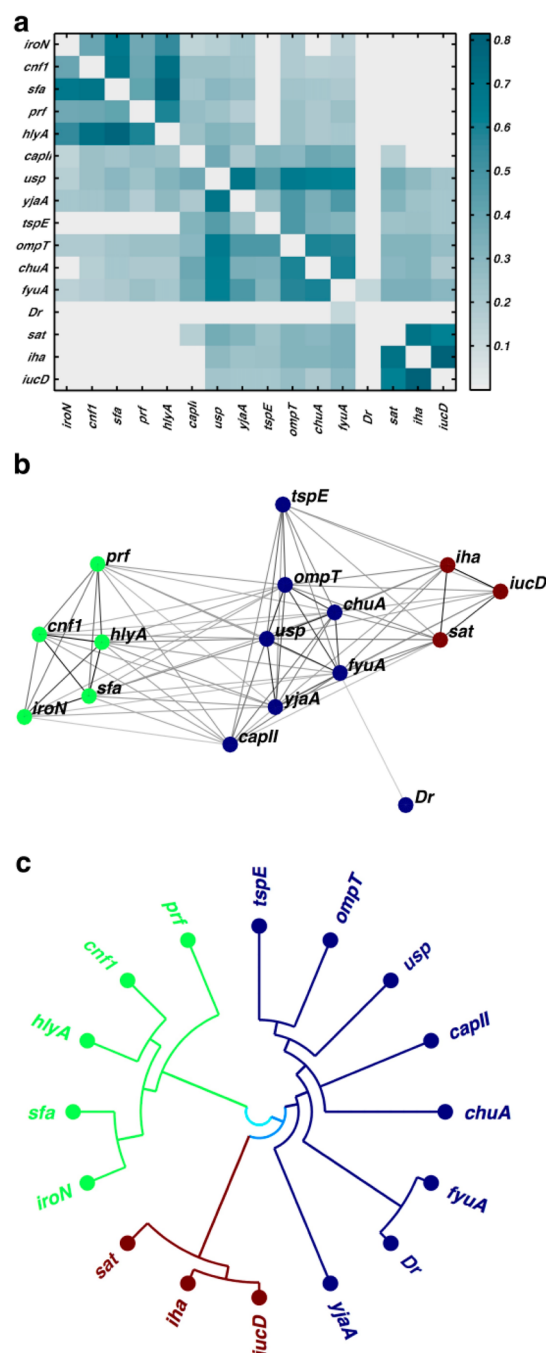


**Figure 2.** Network community detection clusters 16 virulence factors into three discrete communities. (a) Three VF communities are evident in an empirical heatmap depicting statistically significant positive correlations between VFs. (b) A force-directed layout illustrates connectivities between individual virulence factors (VFs) organized into three VF communities (colors). (c) Nested hierarchy of VF genes in a polar coordinate dendrogram are colored according to community identification at default resolution (three communities). Each VF community contains a distinct siderophore gene (*iroN*, *fyuA*, *iucD*).

community 2. By annotating the force-directed layout of the CI strains with bicluster assignments, we reveal many similarities between the two clustering results (Figures 3b and 4b). The stereotypical VF combinations identified by both mathematical approaches define four stereotypical virulence strategists among UPEC in the study population.



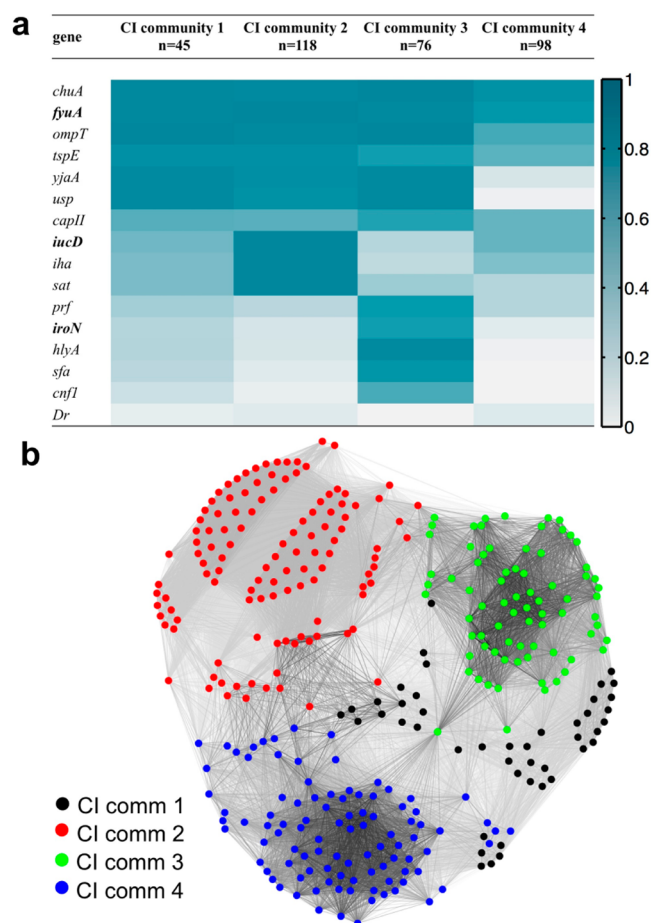


**Figure 3.** Network community detection clusters 337 inpatient clinical isolates into four discrete communities. (a) Four distinct communities (identified using modularity maximization) describe the CIs in this population. Color scale: dark blue, VF presence = 100%; white,  $\leq 5\%$ . (b) A force-directed layout illustrates associations between virulence factor (VF) profiles of individual UPEC clinical isolates (CIs). Each node represents a CI, and connecting line (edge) lengths are determined to most closely match the connectivity level between the connected CIs (colored by CI community assignment).

**Virulence Strategists and Phylogeny.** *E. coli* phylogenetic groups have been used extensively to classify clinical *E. coli* isolates and consistently associate group B2 with extraintestinal infections. We investigated whether CI phylogenetic groups are more informative than the stereotypical VF communities by seeking associations with CI communities and biclusters (Table S1). Assignment to non-B2 phylotypes is associated with C4, BC4, or nonbiclustered strains. Phylogenetic type otherwise exhibited no other clear associations with other VF-defined groupings. These results reveal that the best-resolved virulence strategies represent an organizational level that is distinct from phylogenetic grouping.

**Virulence Strategists and Siderophores.** Network community detection and biclustering each identify collections that possess stereotypical combinations of siderophores, toxins, and adhesins. Among single functional classes, siderophore genotypes effectively distinguish these communities and biclusters from one another. *E. coli* siderophores exhibit diverse structures that likely represent evolutionary adaptive radiation such that one siderophore system may represent a gain of function, whereas another may represent functional redun-

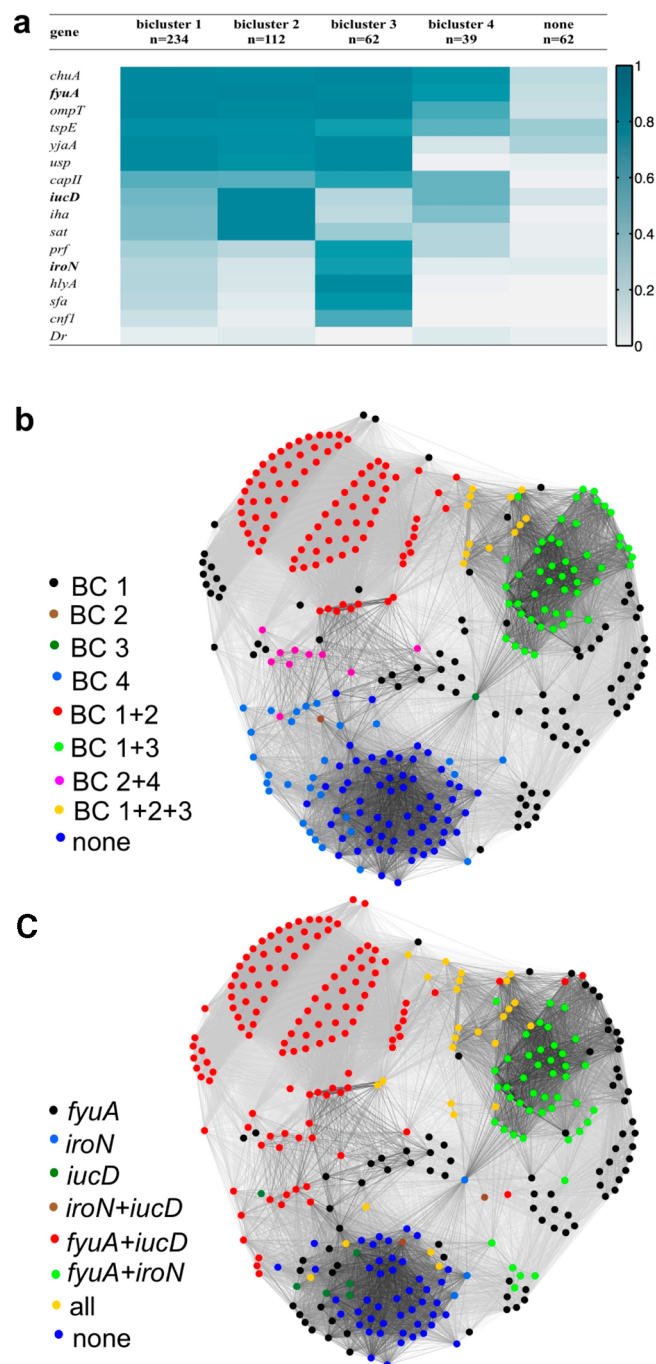


**Figure 4.** Bicluster and siderophore gene composition cluster clinical isolates similarly to network analysis. (a) Four biclusters describe 82% of the CIs in this population. Siderophore genes are in bold type. Color scale: dark blue, VF presence = 100%; white,  $\leq 5\%$ . (b, c) The force-directed layout for clinical isolates overlaid with each CI's bicluster assignments (b) and siderophore genotype (c) illustrates overall similarities between these CI classification approaches and the communities in Figure 1b.

dancy.<sup>25–28</sup> Siderophore systems have also been subject to extensive targeted drug development studies in bacteria.<sup>13,29</sup> We therefore examined siderophore genotypes as an independent way to characterize UPEC strategists. Overlaying siderophore genotypes on the force-directed layout (Figure 4c) reveals this nonrandom siderophore gene distribution. We observed that a representative siderophore genotype character-

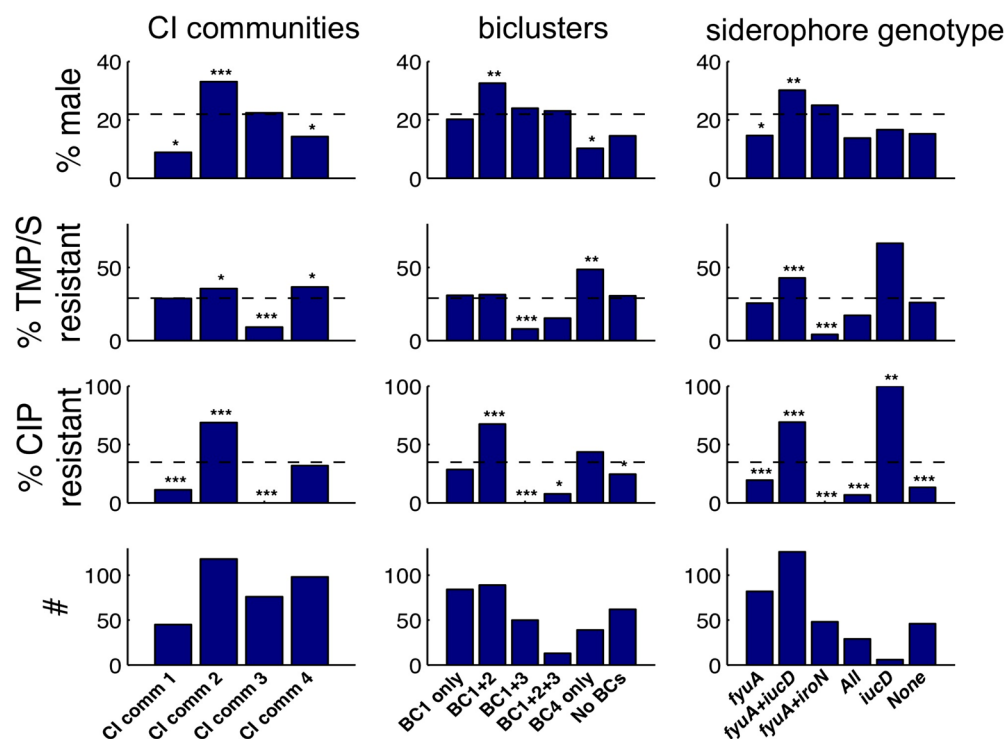


**Figure 5.** CI classifications correspond to antibiotic resistance and patient sex. Patient sex and antibiotic resistance (bars) in each clinical isolate subgroup relative to total study population (dashed lines) are shown. Subgroup size (#) is indicated in the bottom row. Small subgroups (<6 CI) were omitted for clarity. *fyuA+iucD* strategists (community 2, BC1+2) exhibit notable sex and ciprofloxacin resistance associations. Statistical significance determined by Fisher's exact test is indicated by number of asterisks ( $p$  values: 0.05, 0.01, and 0.001, respectively, without correction for multiple testing).

**Table 3. Patient Sex and *E. coli* Virulence Groupings Are Strongly Associated with Ciprofloxacin (CIP) and Trimethoprim/Sulfa (TMP/S) Resistance<sup>a</sup>**

antibiotic	nested multivariate analysis		logistic regression analysis	
	model	deviance	covariate	OR
CIP	sex	415***	male	3.5 (2.0–6.0)***
	sex + CI communities	287***	C2	15.0 (6.0–47.0)***
			male	3.9 (1.9–8.2)***
			C4	4.0 (1.4–11.0)*
	sex + biclusters	322***	male	4.7 (2.4–9.6)***
			BC 1+2	2.1 (1.0–4.7)*
			BC 1	0.4 (0.2–0.9)*
	sex + siderophore genotype	294***	<i>fyuA+iucD</i>	8.0 (5.0–15.0)***
			male	4.1 (2.1–8.6)***
TMP/S	sex	405		
	sex + CI communities	382***	C3	0.2 (0.1–0.4)***
	sex + biclusters	380***	BC 1+3	0.1 (0.0–0.3)***
			BC 1+2+3	0.1 (0.0–0.5)*
			BC 1	0.5 (0.2–0.9)*
			BC 1+2	0.4 (0.2–0.9)*
	sex + siderophore genotype	373***	<i>fyuA+iucD</i>	2.0 (1.4–3.7)**
			<i>fyuA+iroN</i>	0.1 (0.0–0.5)**

<sup>a</sup>In the nested multivariate analyses, lower deviance indicates improved fit to the model. In the logistic regression analyses, odds ratios (OR) of resistance per covariate are shown (with 95% confidence intervals). Only the statistically significant variables from each model are listed for clarity. \*,  $p < 0.05$ ; \*\*,  $p < 0.01$ ; \*\*\*,  $p < 0.00001$ .

izes each CI community (CI community 1 is 88.9% *fyuA* only; CI community 2 is 93.2% *fyuA+iucD*; community 3 is 51.3% *fyuA+iroN*; CI community 4 is 46.9% none). Similarly, representative siderophore genes characterize each BC (BCs 1 and 4 are 61.9% and 34.5% *fyuA* only, respectively; BC 1+2 is

94.4% *fyuA+iucD*; BC 3 is 100% *iroN*). Siderophore genotypes are thus strongly associated with the virulence strategists identified by network community detection and bicluster analysis.

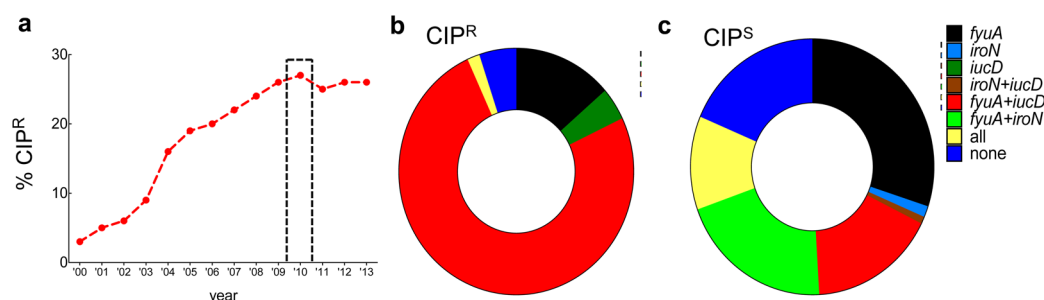


**Figure 6.** Siderophore genotypes as correlates of CIP resistance (CIP<sup>R</sup>). (a) CIP<sup>R</sup> rates among *E. coli* at Barnes-Jewish Hospital from 2000 to 2013 are shown. The gray bar corresponds to the collection period for the clinical isolates examined in this study. (b) Most CIP<sup>R</sup> urinary *E. coli* isolates are *fyuA+iucD* strategists, whereas (c) all *fyuA+iroN* strategists are CIP<sup>S</sup>.

**Virulence Strategists and Patient Sex.** To assess the four virulence strategists' clinical significance, we first investigated associations with patient sex, an organizing principle in UTI medical management. The abundant *fyuA+iucD* strategists (CI community 2, BCs 1+2) are highly associated with male sex (33.1, 32.6, and 30.2%, respectively, compared to the 22% male study population; each deviation is statistically significant as indicated in Figure 5). Female sex, classically a UTI-susceptible population, is predominantly associated with *fyuA* strategists (CI community 1 and BC 4; 8.9 and 10.3% male, respectively). Sex preferences among different virulence strategists may reflect their preferential adaptation to sex-dependent host niches such as the vaginal mucosa, the prostate and its secretions, urethral length, sex differences in immune defenses, hormonal differences, or a combination thereof. These findings suggest that some antivirulence strategies may be particularly useful in a precision medicine context where individual patient factors such as sex guide therapeutic selection.

**Virulence Strategists and Antibiotic Resistance.** To determine whether the four virulence strategists are linked with antibiotic resistance, we investigated associations with phenotypic resistance to the two frequently used oral antibiotics trimethoprim-sulfamethoxazole (TMP/S) and ciprofloxacin (CIP) (Figure 5). The abundant *fyuA+iucD* strategists (CI community 2 and BC 1+2; 68.6 and 73.2% total siderophore genotypes, respectively) are highly associated with CIP resistance and moderately associated with TMP/S resistance (Figure 5). Conversely, the *fyuA+iroN* siderophore genotype (CI community 3, BC 1+3) is highly susceptible to both CIP and TMP/S. These results indicate that virulence strategies are linked to antibiotic responses. Combinatorial targeting of the *fyuA+iucD* siderophore genotype may thus represent an alternative antivirulence strategy against UPEC strains that are resistant to standard antibiotic therapies.

**Multivariate Analysis.** Because virulence strategists were associated with both patient sex and antibiotic resistance (Figure 5), we used nested multivariate logistic regression analyses to determine whether virulence strategies and patient sex contribute independently to antibiotic resistance (Table 3). Incremental addition of VF content to patient sex in the nested model reveals that VF groupings (CI communities, biclusters, or siderophore genotype) are associated independently with antibiotic resistance. To determine which virulence strategists are associated with resistance, we conducted logistic regression analyses with models including each of the three nested strategies. In these analyses, male sex and *fyuA+iucD* siderophore genotype (CI community 2, BC 1+2) are independently associated with CIP resistance, whereas TMP/S resistance

is associated with the *fyuA+iucD* siderophore genotype (but not CI community 2 or BC 1+2). Conversely, the *fyuA+iroN* siderophore genotype (CI community 3, BC 1+3) and BC 1, BC 1+2, and BC 1+2+3 are each strongly associated with TMP/S susceptibility, whereas patient sex is not. Virulence strategies are associated with antibiotic resistance independently of the sex of the patients from whom they were recovered. Targeting specific virulence strategists in this population therefore suggests new treatment strategies for antibiotic-resistant uropathogens.

The contemporary mathematical exploratory tools used here show that *E. coli* VFs tend to exist in stereotypical combinations, which define unique bacterial "strategists", in bacteriuric specimens from a well-characterized patient cohort. Intriguingly, discrete uropathogenic strategists are associated with the clinically important variables of antibiotic resistance and patient sex. These clinical associations suggest that specific VF combinations are worthy of further consideration as combinatorial antivirulence therapeutic targets. Furthermore, the tendency for antibiotic-resistant *E. coli* to carry VF communities associated with yersiniabactin (*fyuA*) and aerobactin (*iucD*) genes suggests new therapeutic targets for uropathogenic isolates in which existing antibiotics are failing.

The striking increase in ciprofloxacin-resistant (CIP<sup>R</sup>) isolates at the study institution over the past 15 years (Figure 6a) parallels the worldwide trend<sup>30</sup> and prompts a closer look at the virulence strategy–CIP<sup>R</sup> association. Mining the extensive literature on worldwide fluoroquinolone resistance in UPEC suggests that the virulence strategists identified in this study may correspond to other geographic locations. In the present study, 75% of CIP<sup>R</sup> isolates possess *fyuA+iucD*, whereas none have the *fyuA+iroN* siderophore genotype (Figure 6b,c). Similar monogenic *E. coli* siderophore correlates of CIP<sup>R</sup> were observed in studies examining nonclonal strains from China, Italy, Iran, Israel, Korea, and Australia.<sup>31–36</sup> Furthermore, when genetically distinct CIP<sup>R</sup> *E. coli* strains (ST131, ST1193, and O15:K52:H1) from geographically distinct locations were characterized by full genome sequencing, aerobactin genes (*iucD*, *iutA*) were present and salmochelin genes (*iroBCDEN*) were absent.<sup>37–39</sup> Interestingly, CIP<sup>S</sup> correlates were correlated with *iroN* expression in studies conducted in India and France.<sup>40,41</sup> Whereas a more systematic international comparison would be more definitive, these results suggest that antivirulence strategies targeting *fyuA+iucD* strategists would be preferentially effective against CIP<sup>R</sup> *E. coli* in geographically diverse populations. This connection between virulence and resistance is unexpected, and the reason for it remains unclear.



The existence of stereotypical virulence strategists across multiple phylogenetic types (the main communities detected here contain both phylogenetic group B2 and non-B2 strains) in bacteriuric isolates suggests an underlying pathophysiologic basis for VF community composition. In the evolutionary paradigm, VFs with complementary activities are expected to possess a selective advantage, whereas a noncomplementary VF may confer a metabolic penalty.<sup>42</sup> Pathogenic success in these bacteria may thus be a more qualitative phenomenon than the sum total of virulence factors alone (the “virulence score”) would suggest. The sex-selective strategists observed here raise the possibility that the *iucD*-associated VF community confers greater fitness for a male pathophysiologic niche such as prostate tissue. It is less clear why the same VF community is associated with antibiotic resistance, although this could be associated with distinctive antibiotic uses in male patients or occupation of a niche that facilitates resistance. Possible contributions from local circulating *E. coli* clones, plasmids, phages, or antibiotic use patterns to the results are also unclear. Much remains to be learned about the biology and therapeutic implications of the combinatorial strategists identified here. Although the VF genes assessed here are almost certainly an incomplete list, application of the mathematical approaches described here to more extensive genetic data from a geographically more diverse patient cohort would help to evaluate the interpretations above.

By resolving meaningful associative patterns from heterogeneous clinical isolates, contemporary exploratory tools such as network analysis offer significant advances over traditional monogenic analyses. Additionally, these approaches are insensitive to additive or synergistic VF combinations that enhance pathogen virulence or antagonistic combinations that reduce it. Whereas network community detection amplifies signal from noise to identify superstructures in the data, the complementary biclustering approach described here simultaneously identifies related *E. coli* strains and virulence factors that significantly interact. By offering a simplified relational superstructure of the data, they also account for the possibility of clonality in a complex pathogenic data set. It is notable that network analysis and biclustering identified VF communities that mirror the evolutionary relationships proposed above. Basically, network analysis identifies VF pairs that are most successful in the study population (i.e., most strongly associated with each other relative to chance) and progressively assembles these into an interrelated network based upon these pairwise interactions. In contrast, more restrictive methods such as PCA and hierarchical clustering (Figures S2 and S3) do not capture the interacting gene groups identified in this study. Analyzed with different tools, the choice of antivirulence targets is thus an extension of their evolutionary interrelationships. Targeting these synergistic combinations would lower selective pressure for antibiotic resistance and minimize the impact on commensal bacteria, presenting a major advance in infection pharmacotherapy.

## METHODS

**Study Design, Data Collection, Laboratory Analyses, and Definitions.** The samples were collected as part of a 1 year (August 1, 2009, to July 31, 2010) Washington University Institutional Review Board-approved prospective study of patients with *E. coli* bacteriuria ( $>5 \times 10^4$  colony-forming units (CFU)/mL) described by Marshall et al.<sup>20</sup> These urine cultures were obtained as part of the clinical workup for these

patients and were then processed at the hospital's medical microbiology laboratory. Clinical isolates were retrieved directly from this laboratory once bacteriuric patients were identified in the hospital's patient database. Strains without associated blood culture data were not excluded from this study. Briefly, clinical isolates were collected from male and female patients with significant bacteriuria. Bacterial DNA was extracted using a QIAamp DNA mini kit (Qiagen, Valencia, CA, USA). DNA probes for virulence genes were developed as previously described<sup>20</sup> by the molecular epidemiology laboratory at the University of Michigan's School of Public Health, and the presence of these genes was determined by dot-blot hybridization using a previously described microarray system<sup>43</sup> (Table 1). This method is based on established cDNA glass microarray fabrication and hybridization techniques that are modified by printing total bacterial genomic DNA on the slide. The hybridization signal is determined by both the target concentration in the spot and the quantity of the fluorescent tag carried by the probe, both of which were empirically optimized by Zhang et al.<sup>43</sup> DNA concentration was controlled for in a separate quantification step, utilizing 16S rRNA PCR. Whereas the clinical isolate collection dates varied, laboratory processing and analysis were concentrated over a small number of defined sessions, each of which included appropriate controls.

The *E. coli* phylogenetic group was determined from hybridization results using the triple genotyping method of Clermont et al.<sup>44</sup> Antimicrobial susceptibility was determined using disk diffusion tests (Kirby–Bauer). In this commonly used test, bacterial growth is observed in response to a standard concentration of a particular antibiotic. Resistance is defined by employing Clinical and Laboratory Standards Institute (CLSI; Wayne, PA, USA) standards for measuring the zone of inhibition around the antibiotic-impregnated disk and comparing it to a standard interpretation chart.<sup>45</sup> Only three isolates qualified as moderately resistant by this measure (the rest were either resistant or susceptible) and were qualified as resistant for the purposes of this study. Bacteriuria was defined as  $\geq 5 \times 10^4$  CFU/mL in noncatheterized patients and  $\geq 5 \times 10^3$  CFU/mL in catheterized patients, as well as by using the patients' documented urinary symptoms. Pyelonephritis was defined as the presence of flank pain and tenderness and/or fever; sepsis and sepsis-induced hypotension were defined using established clinical criteria. The Microbiology Laboratory at Barnes-Jewish Hospital provided clinical antibiogram data.

**Network Analysis.** The (bipartite) clinical-isolates-by-genes binary data array was projected onto two separate (unipartite) network representations, one each for the clinical isolates and for the VFs. The VF network, connected by similar co-occurrences across the clinical isolate population, was defined by statistically significant positive correlation coefficients between VF pairs. Statistical significance was determined by Fisher exact tests on  $2 \times 2$  contingency tables; for each pair of genes the  $2 \times 2$  contingency table of the number of expressed and not-expressed outcomes for each of these two genes was tabulated, and then a Fisher exact test was used to determine whether or not the two genes appeared independently within the population of clinical isolates, conditional on their observed marginal frequencies in the population. A 1.5% *p* value threshold (one-tailed on the right, without correction for multiple testing) was chosen to ensure that the resulting network of VFs was a single connected component. An edge was defined as present between any pair

of positively correlated genes that satisfied the threshold, and then the positive weight of that edge was set by the correlation coefficient. To continue to respect the diversity of background VF expression frequencies, we define the network of clinical isolates in terms of the column-standardized version of the clinical-isolates-by-VFs data array; that is, each column is centered to zero and rescaled to unit variance. The resulting column-standardized matrix  $\mathbf{M}$  yielded the full matrix of correlation coefficients between VFs through the expression  $\mathbf{M}^T\mathbf{M}/(n-1)$ , where  $n$  is the number of clinical isolates. For symmetry, we defined the clinical isolates adjacency matrix, the  $(i,j)$  element of which indicates the presence and weight of the edge connecting nodes  $i$  and  $j$ , from the matrix product  $\mathbf{M}\mathbf{M}^T$ , thresholding the elements to retain all positive elements of the resulting matrix product. We set the diagonals of both adjacency matrices to zero (no self-loops).

Community detection of the clinical isolate and VF networks was performed by maximizing modularity with a resolution parameter, by a generalized implementation of the Louvain method followed by Kernighan–Lin node-swapping steps.<sup>21,22,46,47</sup> Networks were partitioned into various numbers of communities by varying the resolution parameter ( $\gamma$  index, Figure S4). This parameter appears directly in the definition of modularity and optimizes community selection. Through this procedure, a collection of nested VF network partitions was identified (as visualized in the main text). For the network of CIs, closely similar four-community partitions were identified in a range of gamma values straddling its default value ( $\gamma = 1.0$ ), so we restricted our attention to a four-community partition found at that default resolution.

**Biclustering.** Biclustering is a popular statistical tool for exploratory analysis of high-dimensional data.<sup>48</sup> Given a matrix of genes by isolates, the goal of biclustering is to group the rows and columns to find “dense” regions of the matrix, that is, groups of VFs similarly expressed by subsets of isolates. The expression profile is a binary structure where values for each clinical isolate indicate expression of a VF (0 = absence, 1 = presence). A binary version of large average submatrices (LAS) was used to exhaustively search the  $337 \times 16$  condition matrix for all statistically significant biclusters of large average expression.<sup>23</sup>

This method operates in an iterative-residual fashion and is driven by a Bonferroni-based significance score that trades off between submatrix size and average value. The method identified statistically significant large average biclusters, in the sense that the VFs are expressed across the collection of clinical isolates more often than expected within the entire population. The significance of an identified  $k \times l$  bicluster  $U$  is measured through a binary score function

$$S(U) = -\log \left[ \binom{m}{k} \binom{n}{l} F(kl - \tau; kl, 1 - p) \right]$$

where  $F(\tau; kl; 1 - p)$  gives the null probability that the  $kl$  entries of  $U$  have  $\tau$  or more 1s. The probability inside the logarithm is a Bonferroni-corrected  $p$  value associated with observing a submatrix with an average at least as large as  $U$ . The algorithm was set to find biclusters with score  $S(U) \geq 100$ .

**Statistical Analysis.** A multivariate logistic regression model was used to identify covariates significantly associated with antibiotic resistance. The fitted model included indicator (0/1) covariates for sex, community containment, bicluster containment, and siderophore content. The covariates with

statistically significant coefficients ( $p$  value  $< 0.10$ ) for each antibiotic (CIP and TMP/S) are shown in Table 3. A nested models approach was used to determine the significance of variability in antibiotic resistance (CIP and TMP/S) explained by the inclusion of covariates describing sex, community containment, bicluster containment, and siderophore type. The null model contained only the mean response for resistance to CIP and TMP/S, respectively. Sequentially, each of the above covariates was added to the null model, and the variability explained in the model was recorded. To test the significance of the added covariate type, an analysis of deviance was employed wherein a  $\chi^2$  test was used to test the reduction in deviance from the null model. The models and test results are shown in Table 3. PCA and hierarchical analysis were conducted using MATLAB.

## ■ ASSOCIATED CONTENT

### Supporting Information

The Supporting Information is available free of charge on the ACS Publications website at DOI: 10.1021/acsinfecdis.5b00022.

Frequency with which the virulence factors examined in this study are reported in PubMed (figures and tables) (PDF)

Supplemental raw data (PDF)

## ■ AUTHOR INFORMATION

### Corresponding Authors

\*(P.J.M.) E-mail: mucha@unc.edu.

\*(J.P.H.) E-mail: jhenderson@DOM.wustl.edu.

### Present Address

$\Delta$ Department of Mathematics and Statistics, the University of San Francisco

### Notes

The authors declare no competing financial interest.

## ■ ACKNOWLEDGMENTS

We thank B. Foxman and L. Zhang (University of Michigan, Ann Arbor, MI, USA) for dot-blot hybridization analysis. We also thank C. A. Burnham, E. Casabar, and the Barnes-Jewish Hospital Microbiology Laboratory for assistance with clinical isolates and antibiotic resistance records. J.P.H. holds a Career Award for Medical Scientists from the Burroughs-Wellcome Fund and acknowledges NIH Grants R01DK099534 and P50DK064540. J.M. acknowledges NIH Grants UL1RR024992, KL2RR024994, and BIRCWH SK12HD001459-13. J.D.W. acknowledges NSF Grant DMS-1310002. P.J.M. acknowledges support from the James S. McDonnell Foundation 21st Century Science Initiative – Complex Systems Scholar Award Grant 220020315. J.P.H. and K.S.C. additionally acknowledge the Longer Life Foundation and the Center for Women’s Infectious Disease Pilot Research Project Grant.

## ■ REFERENCES

- (1) Dethlefsen, L., and Relman, D. A. (2011) Incomplete recovery and individualized responses of the human distal gut microbiota to repeated antibiotic perturbation. *Proc. Natl. Acad. Sci. U. S. A.* 108 (Suppl. 1), 4554–4561.
- (2) Sekirov, I., Tam, N. M., Jogova, M., Robertson, M. L., Li, Y., Lupp, C., and Finlay, B. B. (2008) Antibiotic-induced perturbations of



the intestinal microbiota alter host susceptibility to enteric infection. *Infect. Immun.* 76, 4726–4736.

(3) Ho, J., Tambyah, P. A., and Paterson, D. L. (2010) Multiresistant Gram-negative infections: a global perspective. *Curr. Opin. Infect. Dis.* 23, 546–553.

(4) Gupta, K., Hooton, T. M., and Stamm, W. E. (2001) Increasing antimicrobial resistance and the management of uncomplicated community-acquired urinary tract infections. *Ann. Intern. Med.* 135, 41–50.

(5) Litwin, M. S., Saigal, C. S., Yano, E. M., Avila, C., Geschwind, S. A., Hanley, J. M., Joyce, G. F., Madison, R., Pace, J., Polich, S. M., and Wang, M. (2005) Urologic diseases in America Project: analytical methods and principal findings. *J. Urol.* 173, 933–937.

(6) Brown, K. A., Khanafer, N., Daneman, N., and Fisman, D. N. (2013) Meta-analysis of antibiotics and the risk of community-associated *Clostridium difficile* infection. *Antimicrob. Agents Chemother.* 57, 2326–2332.

(7) Fischbach, M. A., and Walsh, C. T. (2009) Antibiotics for emerging pathogens. *Science* 325, 1089–1093.

(8) Wiles, T. J., Kulesus, R. R., and Mulvey, M. A. (2008) Origins and virulence mechanisms of uropathogenic *Escherichia coli*. *Exp. Mol. Pathol.* 85, 11–19.

(9) Wandersman, C., and Delepelaire, P. (2004) Bacterial iron sources: from siderophores to hemophores. *Annu. Rev. Microbiol.* 58, 611–647.

(10) Engelhart, C. A., and Aldrich, C. C. (2013) Synthesis of chromone, quinolone, and benzoxazinone sulfonamide nucleosides as conformationally constrained inhibitors of adenylating enzymes required for siderophore biosynthesis. *J. Org. Chem.* 78, 7470–7481.

(11) Lukacik, P., Barnard, T. J., Keller, P. W., Chaturvedi, K. S., Seddiki, N., Fairman, J. W., Noinaj, N., Kirby, T. L., Henderson, J. P., Steven, A. C., Hinnebusch, B. J., and Buchanan, S. K. (2012) Structural engineering of a phage lysin that targets Gram-negative pathogens. *Proc. Natl. Acad. Sci. U. S. A.* 109, 9857–9862.

(12) Zheng, T., and Nolan, E. M. (2014) Enterobactin-mediated delivery of beta-lactam antibiotics enhances antibacterial activity against pathogenic *Escherichia coli*. *J. Am. Chem. Soc.* 136, 9677–9691.

(13) Gorska, A., Sloderbach, A., and Marszall, M. P. (2014) Siderophore-drug complexes: potential medicinal applications of the “Trojan horse” strategy. *Trends Pharmacol. Sci.* 35, 442–449.

(14) Pramanik, A., Stroehrer, U. H., Krejci, J., Standish, A. J., Bohn, E., Paton, J. C., Autenrieth, I. B., and Braun, V. (2007) Albomycin is an effective antibiotic, as exemplified with *Yersinia enterocolitica* and *Streptococcus pneumoniae*. *Int. J. Med. Microbiol.* 297, 459–469.

(15) Cusumano, C. K., Pinkner, J. S., Han, Z., Greene, S. E., Ford, B. A., Crowley, J. R., Henderson, J. P., Janetka, J. W., and Hultgren, S. J. (2011) Treatment and prevention of urinary tract infection with orally active FimH inhibitors. *Sci. Transl. Med.* 3, 109ra115.

(16) Brumbaugh, A. R., Smith, S. N., and Mobley, H. L. (2013) Immunization with the yersiniabactin receptor, FyuA, protects against pyelonephritis in a murine model of urinary tract infection. *Infect. Immun.* 81, 3309–3316.

(17) Langermann, S., and Ballou, W. R. (2003) Development of a recombinant FimCH vaccine for urinary tract infections. *Adv. Exp. Med. Biol.* 539, 635–648.

(18) Clatworthy, A. E., Pierson, E., and Hung, D. T. (2007) Targeting virulence: a new paradigm for antimicrobial therapy. *Nat. Chem. Biol.* 3, 541–548.

(19) Silverman, J. A., Schreiber, H. L. t., Hooton, T. M., and Hultgren, S. J. (2013) From physiology to pharmacy: developments in the pathogenesis and treatment of recurrent urinary tract infections. *Curr. Urol. Rep.* 14, 448–456.

(20) Marschall, J., Zhang, L., Foxman, B., Warren, D. K., Henderson, J. P., and Program, C. D. C. P. E. (2012) Both host and pathogen factors predispose to *Escherichia coli* urinary-source bacteremia in hospitalized patients. *Clin. Infect. Dis.* 54, 1692–1698.

(21) Fortunato, S. (2010) Community detection in graphs. *Phys. Rep.* 486, 75–174.

(22) Porter, M. A., Onnela, J. P., and Mucha, P. J. (2009) Communities in networks. *Notices AMS* 56, 1082–1097, 1164–1066.

(23) Shabalin, A. A., Weigman, V. J., Perou, C. M., and Nobel, A. B. (2009) Finding large average submatrices in high dimensional data. *Ann. Appl. Stat.* 3, 985–1012.

(24) Johnson, J. R., Kuskowski, M. A., Gajewski, A., Soto, S., Horcajada, J. P., Jimenez de Anta, M. T., and Vila, J. (2005) Extended virulence genotypes and phylogenetic background of *Escherichia coli* isolates from patients with cystitis, pyelonephritis, or prostatitis. *J. Infect. Dis.* 191, 46–50.

(25) Chaturvedi, K. S., Hung, C. S., Crowley, J. R., Stapleton, A. E., and Henderson, J. P. (2012) The siderophore yersiniabactin binds copper to protect pathogens during infection. *Nat. Chem. Biol.* 8, 731–736.

(26) Koh, E. I., Hung, C. S., Parker, K. S., Crowley, J. R., Giblin, D. E., and Henderson, J. P. (2015) Metal selectivity by the virulence-associated yersiniabactin metallophore system. *Metallomics* 7, 1011–1022.

(27) Shields-Cutler, R. R., Crowley, J. R., Hung, C. S., Stapleton, A. E., Aldrich, C. C., Marschall, J., and Henderson, J. P. (2015) Human urinary composition controls siderocalin’s antibacterial activity. *J. Biol. Chem.* 290, 15949–15960.

(28) Henderson, J. P., Crowley, J. R., Pinkner, J. S., Walker, J. N., Tsukayama, P., Stamm, W. E., Hooton, T. M., and Hultgren, S. J. (2009) Quantitative metabolomics reveals an epigenetic blueprint for iron acquisition in uropathogenic *Escherichia coli*. *PLoS Pathog.* 5, e1000305.

(29) Brumbaugh, A. R., and Mobley, H. L. (2012) Preventing urinary tract infection: progress toward an effective *Escherichia coli* vaccine. *Expert Rev. Vaccines* 11, 663–676.

(30) Dalhoff, A. (2012) Global fluoroquinolone resistance epidemiology and implications for clinical use. *Interdiscip. Perspect. Infect. Dis.* 2012, 976273.

(31) Luo, Y., Ma, Y., Zhao, Q., Wang, L., Guo, L., Ye, L., Zhang, Y., and Yang, J. (2012) Similarity and divergence of phylogenies, antimicrobial susceptibilities, and virulence factor profiles of *Escherichia coli* isolates causing recurrent urinary tract infections that persist or result from reinfection. *J. Clin. Microb.* 50, 4002–4007.

(32) Piatti, G., Mannini, A., Balistreri, M., and Schito, A. M. (2008) Virulence factors in urinary *Escherichia coli* strains: phylogenetic background and quinolone and fluoroquinolone resistance. *J. Clin. Microbiol.* 46, 480–487.

(33) Moreno, E., Prats, G., Sabate, M., Perez, T., Johnson, J. R., and Andreu, A. (2006) Quinolone, fluoroquinolone and trimethoprim/sulfamethoxazole resistance in relation to virulence determinants and phylogenetic background among uropathogenic *Escherichia coli*. *J. Antimicrob. Chemother.* 57, 204–211.

(34) Kim, C. S., Kim, M. E., Cho, Y. H., Cho, I. R., and Lee, G. (2010) Virulence characteristics and phylogenetic background of ciprofloxacin resistant *Escherichia coli* in the urine samples from Korean women with acute uncomplicated cystitis. *J. Korean Med. Sci.* 25, 602–607.

(35) Johnson, J. R., Kuskowski, M. A., O’Bryan, T. T., Colodner, R., and Raz, R. (2005) Virulence genotype and phylogenetic origin in relation to antibiotic resistance profile among *Escherichia coli* urine sample isolates from Israeli women with acute uncomplicated cystitis. *Antimicrob. Agents Chemother.* 49, 26–31.

(36) Katouli, M., Brauner, A., Haghighi, L. K., Kaijser, B., Muratov, V., and Molloy, R. (2005) Virulence characteristics of *Escherichia coli* strains causing acute cystitis in young adults in Iran. *J. Infect.* 50, 312–321.

(37) Olesen, B., Frimodt-Moller, J., Leihof, R. F., Struve, C., Johnston, B., Hansen, D. S., Scheutz, F., Krogfelt, K. A., Kuskowski, M. A., Clabots, C., and Johnson, J. R. (2014) Temporal trends in antimicrobial resistance and virulence-associated traits within the *Escherichia coli* sequence type 131 clonal group and its H30 and H30-Rx subclones, 1968 to 2012. *Antimicrob. Agents Chemother.* 58, 6886–6895.

- (38) Olesen, B., Scheutz, F., Menard, M., Skov, M. N., Kolmos, H. J., Kuskowski, M. A., and Johnson, J. R. (2009) Three-decade epidemiological analysis of *Escherichia coli* O15:K52:H1. *J. Clin. Microbiol.* 47, 1857–1862.
- (39) Platell, J. L., Trott, D. J., Johnson, J. R., Heisig, P., Heisig, A., Clabots, C. R., Johnston, B., and Cobbold, R. N. (2012) Prominence of an O75 clonal group (clonal complex 14) among non-ST131 fluoroquinolone-resistant *Escherichia coli* causing extraintestinal infections in humans and dogs in Australia. *Antimicrob. Agents Chemother.* 56, 3898–3904.
- (40) Basu, S., Mukherjee, S. K., Hazra, A., and Mukherjee, M. (2013) Molecular characterization of uropathogenic *Escherichia coli*: nalidixic acid and ciprofloxacin resistance, virulent factors and phylogenetic background. *J. Clin. Diagn. Res.* 7, 2727–2731.
- (41) Jaureguy, F., Carbonnelle, E., Bonacorsi, S., Clec'h, C., Casassus, P., Bingen, E., Picard, B., Nassif, X., and Lortholary, O. (2007) Host and bacterial determinants of initial severity and outcome of *Escherichia coli* sepsis. *Clin. Microbiol. Infect.* 13, 854–862.
- (42) Lv, H., Hung, C. S., and Henderson, J. P. (2014) Metabolomic analysis of siderophore cheater mutants reveals metabolic costs of expression in uropathogenic *Escherichia coli*. *J. Proteome Res.* 13, 1397–1404.
- (43) Zhang, L., Srinivasan, U., Marrs, C. F., Ghosh, D., Gilsdorf, J. R., and Foxman, B. (2004) Library on a slide for bacterial comparative genomics. *BMC Microbiol.* 4, 12.
- (44) Clermont, O., Bonacorsi, S., and Bingen, E. (2000) Rapid and simple determination of the *Escherichia coli* phylogenetic group. *Appl. Environ. Microbiol.* 66, 4555–4558.
- (45) CLSI. (2006) *Clinical and Laboratory Standards Institute, M100-S16, Performance Standards for Antimicrobial Susceptibility Testing*, 16th Informational Supplement, Wayne, PA, USA.
- (46) Jutla, I. S., Lucas, G. S., and Mucha, P. J. (2011) A generalized louvain method for community detection implemented in Matlab. <http://netwiki.amath.unc.edu/GenLouvain>.
- (47) Reichardt, J., and Bornholdt, S. (2006) Statistical mechanics of community detection. *Phys. Rev. E* 74, 016110.
- (48) Madeira, S. C., and Oliveira, A. L. (2004) Biclustering algorithms for biological data analysis: a survey. *IEEE/ACM Trans. Comput. Biol. Bioinf.* 1, 24–45.